Phase Retrieval for Spatial-Resolution Measurements of Head-Mounted Displays

Ryan Beams and Chumin Zhao**

*** Center for Devices and Radiological Health, Food and Drug Administration, Silver Spring, MD**

Abstract

We apply phase retrieval methods to simulated spatial resolution measurements of head mounted displays (HMDs) to recover the phase of the light measuring device (LMD). This allows for correctly removing the LMD contributions to the HMD spatial resolution measurements, which was simulated for different LMD and HMD optical aberrations.

Author Keywords

Augmented reality; spatial resolution; metrology; near eye-display; head mounted display

1. Introduction

The image quality of virtual reality (VR) and augmented reality (AR) head mounted displays (HMDs) is critical for many applications including medical [1]. Developing image quality evaluation methods has been a central focus of research and standards development [2-4]. Metrology development has included alignment methods of the light measuring device (LMD) to the HMD [5,6], measuring optical aberrations [7,8], and spatial and temporal resolution [9-12]. Spatial resolution measurements of HMDs have been the subject of considerable research, due to both the importance for applications and the metrology challenges. Several methods have been demonstrated, which has included line spread function and point spread function approaches [our work]. However, a challenge for any spatial resolution evaluation method is that measurements depend on the performance of the LMD. For conventional displays, the contribution of the LMD to the measurements can be removed by independently measuring the spatial resolution of the LMD. The spatial resolution of the display can then be determined by dividing the total system modulation transfer function (MTF_{Total}), including the LMD and the display, by the MTF of the LMD (MTF_{LMD}). While this approach is appropriate for conventional displays, there are challenges for HMDs, because the LMD is effectively part of the optical system and therefore the optical coherence is important. In other words, the HMD and LMD cannot be treated independently, and the optical phase of the total system is important. For LMDs with diffraction limited performance, $MTF_{HMD} = \frac{MTF_{Total}}{MTF_{LMD}}$ is correct, since the LMD does not have any wavefront errors. However, for non-diffraction limited LMDs, the wavefront errors of the LMD and HMD combine, and therefore the phases of each are required to determine the spatial resolution of the total system, LMD, and HMD. Ref [13] showed simulations of the MTF errors for an HMD with pancake lenses and two different LMDs and demonstrated that the simple equation $MTF_{HMD} = MTF_{Total}/MTF_{LMD}$ is in general incorrect.

To illustrate the importance of the phase term, Figure 1a shows an example measurement system. In the diffraction limited case, shown in the top part of Figure 1b, plane waves from the HMD are focused by the LMD onto the sensor and the contribution of the LMD is straight forward to remove. In the bottom part of Figure 1b, the HMD and the LMD have optical aberrations that add coherently to produce the final spatial resolution

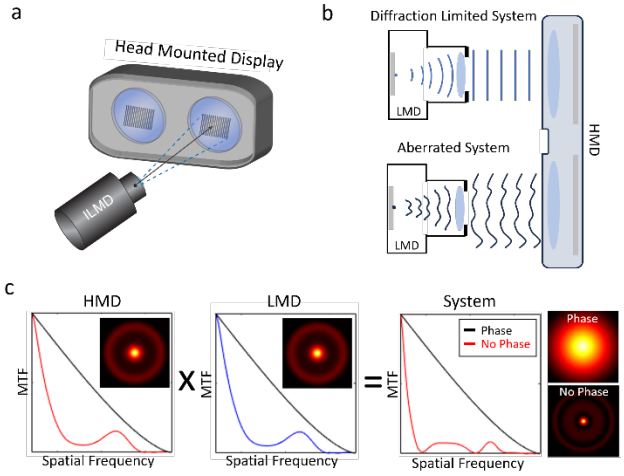

Figure 1. a. Sketch of a head mounted display image quality measurements using light measuring device (LMD) b. Top row: Illustrations of wavefronts of diffraction limited HMD and LMD. Bottom row: Aberrated wavefronts from and HMD and LMD, which both contribute to the resulting spatial measurement. c. Example calculated system MTF with and without the phase contributions to the MTF, shown in blue and red, respectively.

measurement. Since the sensor measures the intensity of the incident field, the phase term is not measured and therefore removing the impact of the LMD is difficult. As an example, Figure 1c shows the MTF_{HMD} (red line) and the MTF_{LMD} (blue line) are the same, but phases are opposite. The diffraction limited MTF is shown as a reference (black line). The results of simply dividing the MTFs compared to including the phase terms are shown in red and black, respectively. In this case, the optical aberrations of the LMD and HMD cancel resulting in a total system MTF significantly better than either MTF_{LMD} or MTF_{HMD}. Therefore, for non-diffraction limited system, the phase of the LMD and HMD are important.

While the wavefront errors or optical phase are frequently measured for single lenses using interferometric techniques, this approach is not feasible for complex HMDs. However, alternative methods have been developed to recover the phase through iterative algorithm methods using prior knowledge of the object and optical system. One common method is known as phase retrieval and has been used for applications including characterizing the optical aberrations of the Hubble space telescope [14-16].

In this work, we demonstrate a method for determining the optical phase of the LMD and HMD by applying phase retrieval algorithms. This allows for separating the LMD contribution to the spatial resolution measurements to determine the HMD performance even with an LMD with optical aberrations. The results show simulations of the HMD spatial resolution measured using LMDs with different known optical aberrations and

ISSN 0097-996X/25/5603-2321-$1.00 © 2025

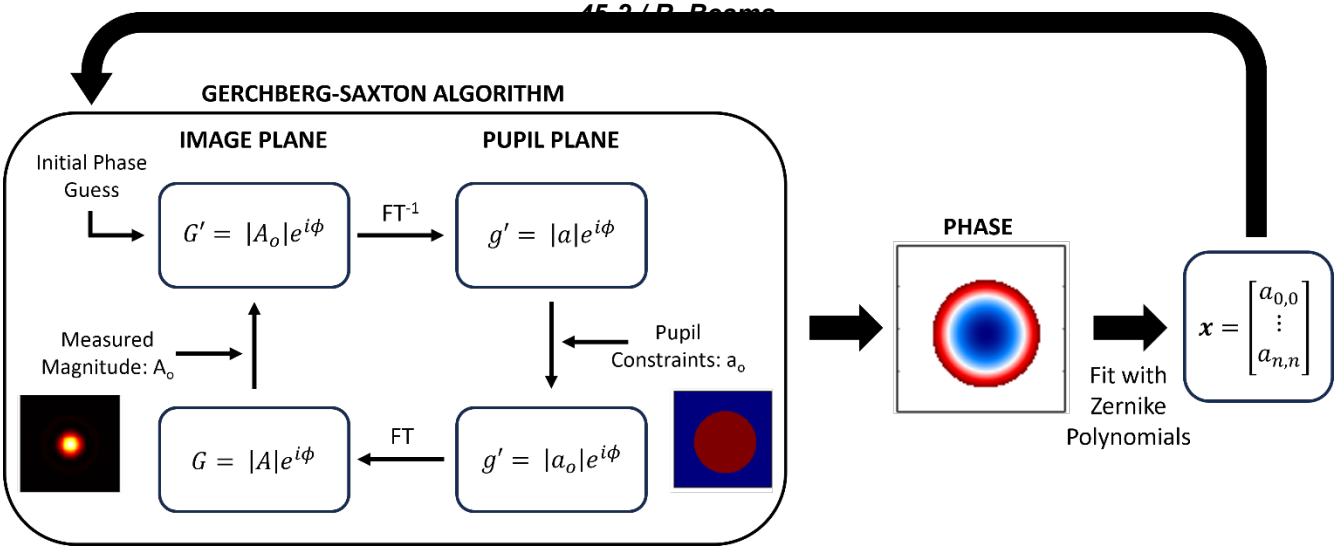

Figure 2. Phase retrieval algorithm method. The G-S algorithm is used to retrieve the phase based on the measured amplitude and system constraints. The output phase is then fit with Zernike polynomials to decompose the phase into optical aberrations, which is used to seed the initial phase guess for the G-S algorithm.

demonstrates that this method can determine the HMD spatial resolution.

2. Methods

Phase Retrieval:

Figure 2 shows the phase retrieval method used in this work based on the Gerchberg-Saxton (G-S) algorithm [14,15,17]. For the G-S algorithm, the amplitude of the image is used as an input. In our case this is magnitude of the point spread function (PSF), $|A_o(x,y)|$, which is multiplied by an initial guess for the phase, $\phi(x,y)$. We used a uniform phase as the initial guess. The resulting complex function, $G'(x,y)$, was Fourier transformed to generate the complex function in the pupil plane, $g'(f_x,f_y)$. The amplitude in the pupil plane was replaced by the known constraints of the system, namely a pupil of known size with uniform illumination, $|a_o(f_x,f_y)|$. Physically this requirement means the LMDs aperture size is known and the optical field from the HMD has uniform intensity across the LMD aperture and there is no light leakage outside the aperture. The new pupil function is Fourier transformed back to the image plane and the amplitude is replaced again by $|A_o(x,y)|$. This iteration is repeated until the solution converges with the necessary phase.

To ensure the results are physical, the resulting phase term was subsequently decomposed into the orthogonal basis set of Zernike polynomials that represent the optical aberrations. Mathematically, wavefront errors, $W(\rho,\varphi)$, can be represented as a sum of Zernike polynomials, $Z_n^m(\rho,\varphi)$, in radial coordinates using the equation, $W(\rho,\varphi) = \sum_{n,m} Z_n^m(\rho,\varphi)$, where n and m indicate the order of the polynomial and ρ and φ are the normalized radial coordinates in the pupil plane. In matrix format, we can write the equation $\boldsymbol{Ax} = \boldsymbol{b}$, where

$$\boldsymbol{A} = \begin{pmatrix} Z_0^0(\rho_1,\varphi_1) & \cdots & Z_n^n(\rho_1,\varphi_1) \\ \vdots & \ddots & \vdots \\ Z_0^0(\rho_N,\varphi_N) & \cdots & Z_n^n(\rho_N,\varphi_N) \end{pmatrix}, \quad (1)$$

$$\boldsymbol{x} = \begin{bmatrix} a_{0,0} \\ \vdots \\ a_{n,n} \end{bmatrix}, \quad (2)$$

$$\boldsymbol{b} = \begin{bmatrix} W(\rho_1,\varphi_1) \\ \vdots \\ W(\rho_N,\varphi_N) \end{bmatrix}. \quad (3)$$

The resulting phase from the G-S method is $\boldsymbol{b}$, which can be decomposed into the Zernike coefficients using,

$$\boldsymbol{x} = [\boldsymbol{A}^T\boldsymbol{A}]^{-1}\boldsymbol{A}^T\boldsymbol{b}.$$

The resulting coefficients, $\boldsymbol{x}$, can then be used to determine the initial phase guess for the G-S algorithm and repeating the phase retrieval. Iterating between the Zernike fitting and the G-S algorithm improves both the convergence of the phase retrieval and ensures the results are physical.

Figure 3a,b show examples of the PSF and pupil phase terms

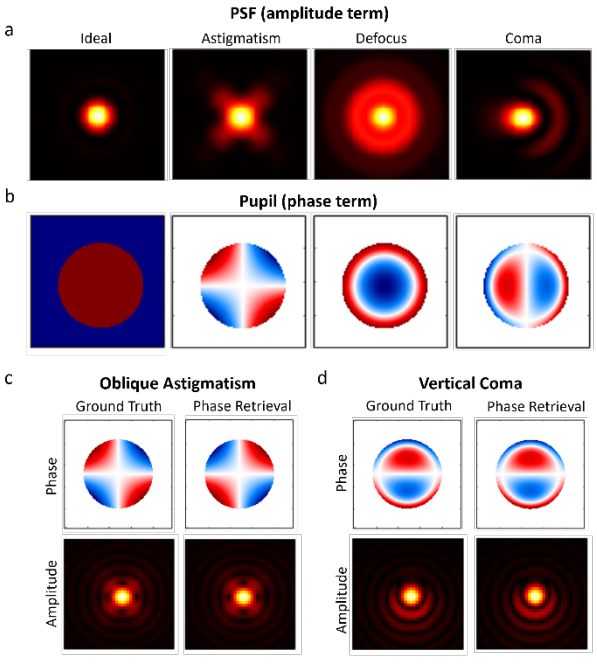

Figure 3. a. PSF amplitude and b. pupil phase term showing ideal diffraction limited, astigmatism, defocus, and coma optical aberrations. c., d. Ground truth and phase retrieval results for oblique astigmatism and vertical coma.

using Zernike polynomials for different optical aberrations. Figure 3 c,d show examples using the phase retrieval method in Figure 2 for oblique astigmatism and vertical coma, respectively, where the PSF amplitude was used for $|A_o|$. The phase retrieval method successfully recovers the phase, demonstrating that the pipeline produces the intended results in this simple case.

For actual spatial resolution measurements, the method is repeated for both the LMD and for the HMD system. This is accomplished by using the measured PSF of the total system (LMD and HMD) and the LMD PSF measurements. This allows for determining both the phase of the LMD and the total system. The phase of the HMD is then determined by taking the difference of the LMD and system phases. It is important to note, that the G-S algorithm has a sign ambiguity, which means the results of the process discussed gives two solutions for the HMD phase. The phase ambiguity can be resolved by repeated measurements, which will be discussed later.

3. Results

The phase retrieval method was tested by simulating an HMD measured with LMDs with different optical aberrations. Since the results are simulated, the amplitude and phase of each component are known, and the pipeline is tested to determine if this known phase can be recovered. Figure 4a, b shows the ground truth for the amplitude, pupil phase, and MTF for the LMD and HMD, respectively. LMDs with different optical aberrations were used in the simulation, namely diffraction limited (ideal), oblique astigmatism, horizontal coma, spherical, and a mixture of several aberrations (mixed). The same optical aberrations for the HMD were used in each simulation. The results of the phase retrieval for the LMD and HMD are shown in Figure 4c. The resulting image amplitudes, pupil phases, and MTFs are in good agreement with the ground truth shown in

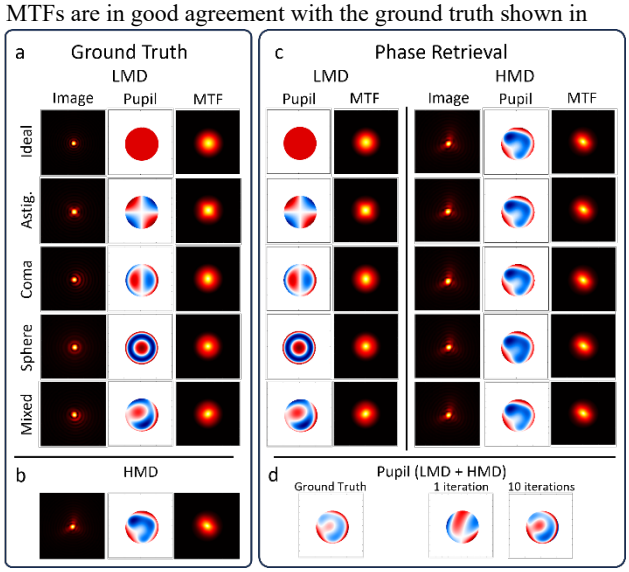

Figure 4. Examples of phase retrieval method applied to a simulations of HMD measurements using LMDs with different optical aberrations. a. Ground truth image amplitude, pupil phase, and MTF for the LMD. b. Ground truth image amplitude, pupil phase, and MTF of the HMD. c. Phase retrieval results for the LMD and HMD with the optical aberrations shown in **a**. d. Pupil phase for the entire system, LMD + HMD, for the ground truth, after 1 iteration, and 10 iterations of the phase retrieval method.

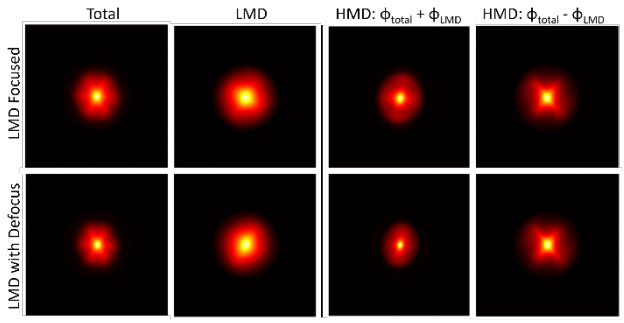

Figure 5. Example MTF calculations from the phase retrieval method with an LMD that is focused and defocused. The $\boldsymbol{MTF_{HMD}}$ with the phase difference (ϕ_{total} - ϕ_{LMD}) is the same for both defocus values of the LMD.

Figure 4a,b. The pupil phase after 1 and 10 iterations are shown in Figure 4d. It is important to note that in these simulations, the LMD has similar performance to the HMD, which is a more challenging case than the measurements using an LMD with significantly better spatial resolution than the HMD, as recommended [3].

As discussed earlier, there is a sign ambiguity in the phase of the G-S algorithm. Since the MTF and image amplitude are the modulus of the signal, the sign of the phase does not impact the results. However, since the phase of the LMD can be either added or subtracted from the total system, there are two potential solutions. However, this can be addressed by repeating the process with two different defocus amounts for the LMD. This results in four potential solutions with two solutions being identical, which is therefore the correct solution. Figure 5 shows an example of the calculated MTF where the pupil phase of the LMD has been added and subtracted from the total phase of the system. Notice that the MTF_{HMD} is the same for the two LMD defocus values for the phase difference case, meaning this is the correct result (right column).

Figure 6 shows examples of the MTF profile for the astigmatism and mixed cases in Figure 4. The ideal diffraction limited MTF is shown in black. The ground truth for the LMD and HMD are shown in red and blue solid lines, respectively. The results from the phase retrieval method for the LMD (red dashed line) and HMD (blue dashed line) are in excellent agreement with the ground truth for both the astigmatism and mixed cases. As a comparison, the MTF of the HMD was also calculated using the equation, $MTF_{HMD} = MTF_{Total}/MTF_{LMD}$, without including the phase term, which is shown in green. While the phase retrieval method accurately calculates the MTF_{HMD}, ignoring the

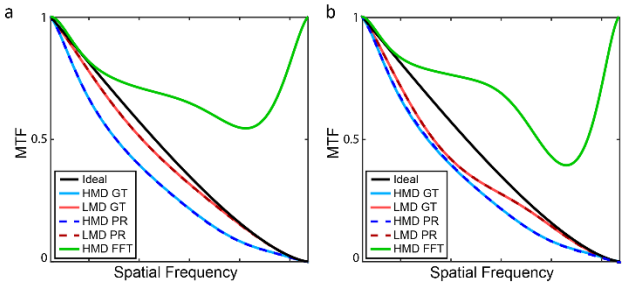

Figure 6. MTF profile showing the ideal (black), LMD (blue), and HMD (red) for the ground truth (solid lines) and the phase retrieval method (dashed lines). a. astigmatism. b. mixed.

phase term results in significant MTF errors. These results show that the phase retrieval method discussed is a promising method for determining the MTF and spatial resolution of an HMD even with an aberrated LMD.

4. Conclusion

In this work we demonstrated that phase retrieval methods can be applied to spatial resolution measurements of HMDs to correctly remove the contribution of the LMD to the measurement. This is accomplished by recovering the phase of the LMD and total system to determine the phase of the HMD, which allows for correctly calculating the HMD PSF and MTF. The results presented were simulated and future work will apply this method to experimental measurements to test the impact of noise and pixelation on the method. We think this method provides a potential pathway to address the current challenges in spatial resolution measurements of HMD.

5. Acknowledgements

The mention of commercial products, their sources, or their use in connection with material reported herein is not to be construed as either an actual or implied endorsement of such products by the Department of Health and Human Services.

6. References

1. Beams R, Brown E, Cheng WC, Joyner JS, Kim AS, Kontson K, Amiras D, Baeuerle T, Greenleaf W, Grossmann RJ, Gupta A. Evaluation Challenges for the Application of Extended Reality Devices in Medicine. Journal of Digital Imaging. 2022 Apr 25:1-0.
2. IEC 63145–20-20:2019. Eyewear display – part 20–20: fundamental measurement methods – image quality. Int Electrotech Comm. 2020.
3. International Committee for Display Metrology (ICDM), Information display measurements standards, March 2022, SID.
4. Beams R, Zhao C, Badano A. Image quality characterization of near-eye displays. Journal of the Society for Information Display. 2024.
5. Draper RS, Penczek J, Varshneya R, Boynton PA. 72-2: Standardizing Fundamental Criteria for Near Eye Display Optical Measurements: Determining Eye Point Position. In SID Symposium Digest of Technical Papers 2018 May (Vol. 49, No. 1, pp. 961-964).
6. Bader AM, Badano A, Beams R. Quadrant detector-based method for eye point alignment of augmented and virtual reality head mounted displays. In Optical Architectures for Displays and Sensing in Augmented, Virtual, and Mixed Reality (AR, VR, MR) III 2022 Mar 7 (Vol. 11931, pp. 82-88). SPIE.
7. Beams R, Kim AS, Badano A. Transverse chromatic aberration in virtual reality head-mounted displays. Optics express. 2019 Sep 2;27(18):24877-84.
8. Penczek J, Hasan M, Denning BS, Calpito R, Austin RL, Boynton PA. 31-2: Measuring Interocular Geometric Distortion of Near-Eye Displays. In SID Symposium Digest of Technical Papers 2019 Jun (Vol. 50, No. 1, pp. 430-433).
9. Beams R, Collins B, Kim AS, Badano A. Angular dependence of the spatial resolution in virtual reality displays. In 2020 IEEE Conference on Virtual Reality and 3D User Interfaces (VR), 2020 (pp. 836-841). IEEE.
10. Johnson M, Zhao C, Varshney A, Beams R. Quantifying the optical and rendering pipeline contributions to spatial resolution in augmented reality displays. Journal of the Society for Information Display. 2024.
11. Zhao C, Kim AS, Beams R, Badano A. Spatiotemporal image quality of virtual reality head mounted displays. Scientific Reports. 2022 Nov 24;12(1):1-3.
12. Masaoka K. 52-4: Simulation of Dynamic MTF Measurement Method for Pixelated Displays. In SID Symposium Digest of Technical Papers 2021 May (Vol. 52, No. 1, pp. 721-724).
13. Winters D, Ruprecht A, Erichsen P, Yadav M, Eggers JH, Stauss B. 82-3: Optical Quality Requirements for Accurate MTF/CTF Measurements on Near-Eye-Displays. In SID Symposium Digest of Technical Papers 2024 Jun (Vol. 55, No. 1, pp. 1147-1150).
14. Gerchberg RW and Saxton W0. A Practical Algorithm for the Determination of Phase from Image and Diffraction Plane Pictures. Optik. 1972. 35, 237.
15. Fienup JR. Phase retrieval algorithms: a comparison. Applied optics. 1982 Aug 1;21(15):2758-69.
16. Fienup JR, Marron JC, Schulz TJ, Seldin JH. Hubble Space Telescope characterized by using phase-retrieval algorithms. Applied optics. 1993 Apr 1;32(10):1747-67.
17. Musa A. Gerchberg–Saxton Algorithm (https://www.mathworks.com/matlabcentral/fileexchange/65979-gerchberg-saxton-algorithm), MATLAB Central File Exchange. Retrieved November 29, 2024.